Nanocomposites Catalysts for Sustainable Chemistry and Environmental Protection

ESFIR M. SULMAN, VALENTINA G. MATVEEVA, MIKCHAIL G. SULMAN, IRINA P. SHKILEVA.
Department of Biotechnology and Chemistry
Tver Technical University
170026, Tver, A.Nikitina st., 22
RUSSIA
sulman@online.tver.ru

Abstract: This report is devoted to the investigation of noble metal nanoparticles formation and stabilization by polymeric nanostructures as well as catalytic properties of synthesized systems. The following types of nanostructured polymers were used: amphiphilic block-copolymers; polyelectrolytes and polymeric matrices. Catalytic properties of nanocomposites were studied in selective hydrogenation of acetylene alcohols, direct selective oxidation of monosaccharides and phenol catalytic wet air oxidation (CWAO). All the catalysts revealed high activity, selectivity (up to 98–99% at 100% conversion) and stability.

The special attention is paid to use of nanocomposites catalysts for environmental protection. CWAO of phenols is an important process of environmental catalysis, allowing one to reach nearly complete oxidation of phenols to non-hazardous compounds. Catalysts based on Ru-containing nanoparticles (NPs) formed in the pores of hypercrosslinked polystyrene (HPS) were synthesized. The catalysts containing from 0.5 to 2.8 wt.% of Ru were studied by transmission electron microscopy (TEM) and X-ray photoelectron spectroscopy (XPS). The NP sizes were controlled by the pores of HPS. The two types of Ru species: Ru(IV) and Ru(IV)×nH_2O, constituted the NP composition. The effects of the phenol initial concentrations and temperature were investigated in the phenol CWAO. Removal of 97% of phenol was observed for the most active catalyst containing 2.8 wt.% of Ru.

Key-Words: nanocatalysis; nanostructured polymers; noble metal nanoparticles; hydrogenation; oxidation, phenol catalytic wet air oxidation

1 Introduction

The main goal of constructing and maintaining an innovative economic model requires the use and development of nanotechnologies, as they can be used to create new economically competitive goods. On the other hand, the general discussion on the prospective implementation of nanosystems seems to be groundless and unreasonable; however, it is necessary to indicate the industrial branches and directions where the application of nanosystems is of certain value. For chemistry and chemical technology, such a branch is certainly represented by metal complex catalysis.

Metal nanoparticles (NPs) have unique catalytic properties due to high number of surface atoms, leading to a high number of reactive sites [1, 2]. Catalytic properties of NPs depend on their size, size distribution and environment [3]. Formation of NPs in nanostructured polymeric environment allows control over NP size and size distribution; in so doing, the stabilizing polymer may strongly influence the surface of NPs [4, 5].

There are several major approaches to stabilize metal nanoparticles by polymers [6 – 9], which were used in this investigation: (i) Formation of metal NPs into the cores of amphiphilic block-copolymer micelles of poly(ethylene oxide)-*block*-poly(2-vinylpyridine) (PEO-*b*-P2VP) and polystyrene-*block*–poly(4-vinylpyridine) (PS-*b*-P4VP); (ii) formation of metal NPs in ultra thin polyelectrolyte (PE) layers (polydiallyldimethyl ammonium chloride (PDADMAC) and biopolymer – chitosan (CS)); (iii) formation of metal NPs into the cavities (pores) of hyper-crosslinked polymeric matrices (hypercrosslinked polystyrene (HPS)).

Both mono- (Pd, Pt, Ru, Au) and bimetallic (Pd-Au, Pd-Pt, Pd-Zn) nanostructured polymer-stabilized catalytic systems were synthesized and investigated in several reactions of fine organic synthesis of both fundamental and industrial importance: selective hydrogenation of triple bond of acetylene alcohols (i.e. dehydrolinalool (DHL)); direct oxidation of monosaccharides (e.g. D-

glucose). Besides, the reaction of environmental importance was studied: phenol catalytic wet air oxidation (CWAO).

Selective hydrogenation of long-chain acetylene alcohols is a key stage of intermediates of vitamin E, K and β-carotene production. Besides, the product of DHL hydrogenation – olefin alcohol linalool (LN) – is a fragrance substance, a part of perfumes, and also shows antimicrobic activity. In this case dihydrolinalool (DiHL) is the side product (Fig. 1).

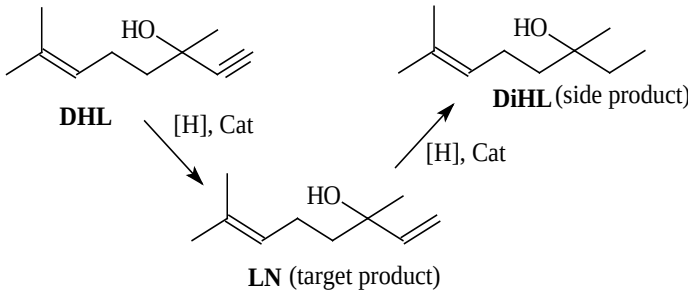

Fig. 1. Scheme of DHL hydrogenation.

Oxidation reaction of D-glucose to D-gluconic acid is used for the industrial synthesis of vitamins B_2, B_{15} and calcium gluconate (Fig. 2). Several methods are used for the oxidation of monosaccharides. However, for the existent technologies, the catalytic oxidation is carried out with a number of complications (e.g. protection and deprotection of functional groups). The use of a selective catalyst would allow for increasing the production, reduction of expenses and improving of the target product quality.

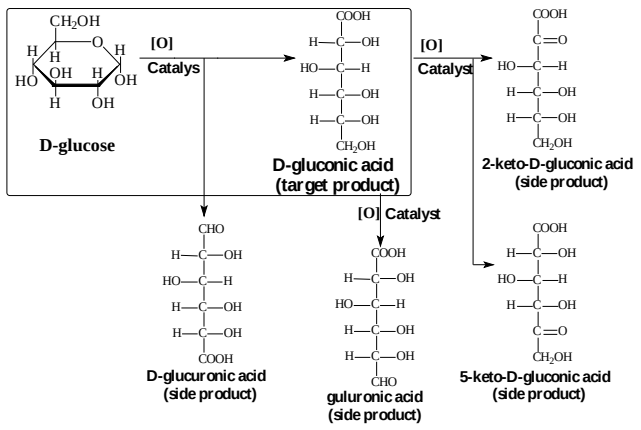

Fig. 2. Scheme of D-glucose oxidation (the possible side products are shown).

Nowadays there is a large amount of organic pollutants in the noosphere, hence, novel technologies based on the conversion of organic pollutants to non-hazardous or useful substances should be developed [10-11]. CWAO is one of the most popular methods for treatment of wastewater containing high concentrations of extremely toxic organic compounds [11-20]. The use of the catalyst accelerates the oxidation rate and reduces waste concentration to the level at which the sewage can be used for technological needs [21, 22]. Phenol is a typical pollutant and frequently used as a model substrate for evaluation of the catalyst activity in the catalytic wet air oxidation [11, 15, 23]. Phenol oxidation is rather a complex process (Fig. 3), where the catalyst activity is a key factor to achieving complete oxidation of phenol to nonhazardous or easily biodegradable products. Another challenge is to design a highly selective catalyst comprising of active sites with a correct ensemble of metal atoms and other active components [24, 25].

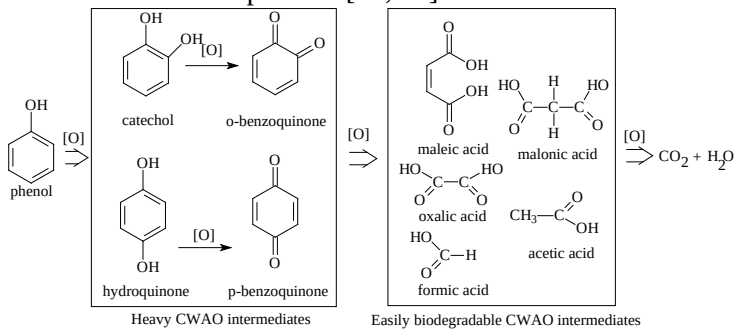

Fig.3 Scheme of phenol wet air oxidation

The key to the successful application of the CWAO process is to develop a heterogeneous catalyst because of the stability of such catalysts compared to homogeneous or colloidal ones. On the other hand, it is already well established that metal or metal oxide nanoparticles (NPs) possess higher activity than conventional heterogeneous catalysts due to large surface areas and numerous active sites [26-28]. As was demonstrated, the presence of nanostructures in polymers allows one to control the growth of nanoparticles, the particle size distribution and interfacial interactions and therefore to control the catalytic properties [22, 25, 29]. Nanoporous polymers are the example of the polymer nanostructures. Nanopores can work as nanoreactors for NP formation.

This paper is devoted to the investigation of noble metal nanoparticles formation and stabilization by polymeric nanostructures as well as catalytic properties of synthesized systems. The following types of nanostructured polymers were

used: amphiphilic block-copolymers; polyelectrolytes and polymeric matrices. Catalytic properties of nanocomposites were studied in the selective hydrogenation of acetylene alcohols, direct selective oxidation of monosaccharides and phenol catalytic wet air oxidation (CWAO). All the catalysts revealed high activity, selectivity (up to 98–99% at 100% conversion) and stability.

2 Experimental

2.1 Catalysts Preparation

2.1.1 Catalytic NPs Stabilized into the Micelle Cores of Amphiohilic Block Copolymers

To synthesize nanocatalysts on the basis of metal NPs stabilized into the micelles of amphiphilic block copolymers it is necessary to provide the presence of functional groups, which are able to react with metal compounds to form complex or salt, in one of the blocks. If this block is the component of micelle core the latter can be filled with corresponding metal and used as nanoreactor for nanoparticles formation. P4(2)VP was found to be the block, which can effectively retain growing metal NPs due to the existence of nitrogen electronic doublet. Micelle crown should consist from the block, which doesn't contain any functional groups but provides the solubility and stability of the micelle in corresponding solvent. Besides, the choice of reducing agent directly influences the size and morphology of synthesized NPs (Fig. 4).

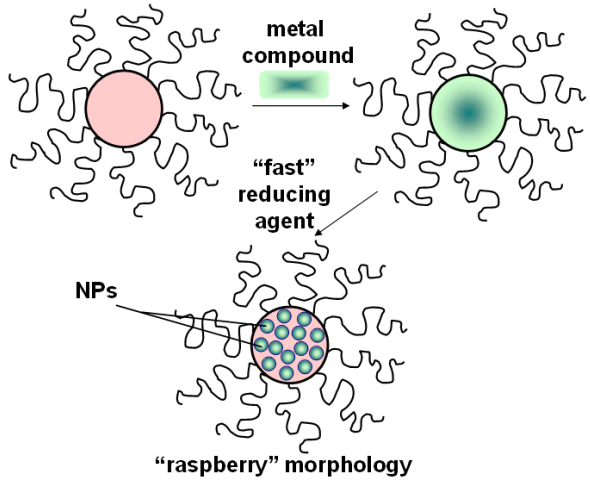

Fig. 4. Scheme of NPs formation into the micelle cores of amphiphilic block copolymers.

Thus, micellar catalysts were prepared using poly (ethylene oxide)-block-polyvinylpyridine (PEO-b-P2VP) and polystyrene-block-poly-4-vinylpyridine (PS-b-P4VP) as was earlier described elsewhere [5, 6, 8]. Mono- (Pd and Pt) and bimetallic (Pd-Au-, Pd-Pt- and Pd-Zn) catalysts were synthesized by solubilization of appropriate metal salts into vinyl pyridine cores of micelles. Besides, to provide better technological performance of synthesized micellar catalysts the heterogenization was carried out via deposition of metal-containing micelles on γ-Al_2O_3 [30].

2.1.2 Catalytic NPs Stabilized in Ultra Thin PE Layers

PEs are well known to form ultra thin layers on various supports [31, 32]. Both PEs used for NPs stabilization (PDADMAC and CS) are polycations containing nitrogen, which provides the affinity to metal ions.

It is noteworthy that PEs can be deposited on inert support (alumina in particular) using two methods: monolayered and "layer-by-layer" deposition (Fig. 5).

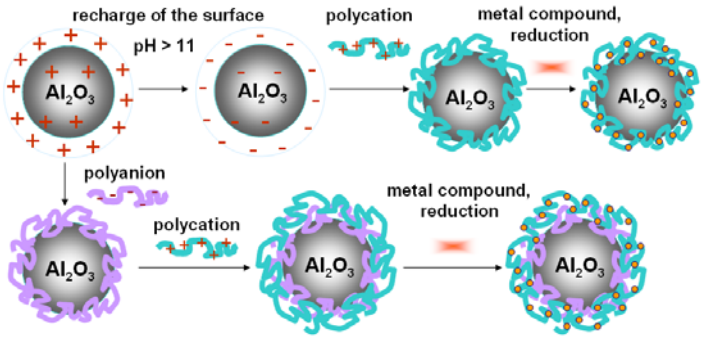

Fig. 5. Scheme of NPs formation in ultra thin PE layers: monolayered and "layer by layer" deposition methods.

For CS-containing catalysts both deposition techniques were used, while for PDADMAC only the monolayered deposition was studied. To provide negative charge on the alumina surface during the one-time deposition of polycations PDADMAC or CS the initial alumina was treated with alkali aqueous solution or (in the case of "layer-by-layer" deposition) with the oppositely charged polyelectrolyte, poly(sodium-4-styrenesulfonate) (PSS) in particular [7]. Depositing the isolating layers of polyanion may regulate the interaction between the NPs-containing layers. Table 1 shows the characteristics of synthesized PE catalysts.

2.1.3 Catalytic NPs Stabilized Into the Bulk of Polymeric Matrix

The use of polymeric matrices as organic supports in catalysis allows controlling the

processes of particles nucleation and growth due to the existence of nanosized voids with high degree of monodispersion [33]. Thus, the series of the catalysts containing mono- (Pd, Pt, Ru) and bimetallic (Pd-Pt, Pd-Zn) noble metal NPs was synthesized on the basis of HPS by the impregnation method as described elsewhere [34].

Table 1. Characteristics of PE catalysts

Catalyst	Pd loading, % (wt.)	Polycation content, g/l	Polyanion (PSS) content, g/l
Pd-PDADMAC	0.580	5.0	-
Pd-CS	0.370	5.0	-
Pd-PSC-1	0.228	5.0	5.0
Pd-PSC-2	0.298	1.0	5.0
Pd-PSC-3	0.300	1.0	1.0
Pd-PSC-4	0.253	0.5	5.0
Pd-PSC-5	0.224	0.5	0.5

2.2 Catalytic Testing

Hydrogenation of DHL was carried out at ambient pressure in a glass batch isothermal reactors installed in a shaker and connected to a gasometric burette. In the case of micellar catalysts various solvents providing the better swelling of micelle corona and access of the substrates to catalytic sites were used (toluene, iPrOH, water). The oxidation of monosaccharides, as well as phenol CWAO were conducted batchwise in PARR apparatuses. The samples of the reaction mixtures were periodically removed for GC or HPLC analysis.

TEM of the HPS based catalysts was performed with a JEOL JEM1010 electron microscope operated at accelerating voltage of 80 kV. Metal-containing HPS powders were embedded in epoxy resin and subsequently microtomed at ambient temperature. Images of the resulting thin sections (*ca*. 50 nm thick) were collected with the Gatan digital camera and analyzed with the Adobe Photoshop software package and the Scion Image Processing Toolkit.

X-ray photoelectron spectra were obtained using Mg Kα ($h\nu$ =1253.6 eV) monochromatized radiation with a modified ES-2403 electron spectrometer equipped with a PHOIBOS 100-5MCD energy analyzer (SPECS, Germany) and an XR-50X-radiation source.

All data were acquired at an X-ray power of 200 W and an energy step of 0.1 eV. The electron-flood gun accessory was used so that the current of the total emitted electron flux from the flood-gun. Samples were allowed to outgas for 30 min before analysis and were sufficiently stable during examination. Data analysis was performed using a standard XPS-set with Resolver program. Identification of band components was achieved by assuming that the Ru $3p_{1/2}$ and $3p_{3/2}$ spin-orbit components (i) exhibit a Gaussian peak shape, (ii) are in 3:2 peak area ratio, and (iii) are separated by 4.1 eV. Surface compositions were discerned by measuring the peak-area intensities of different Ru species.

3 Results and discussion

3.1 Selective Hydrogenation of Acetylene Alcohols

The results of DHL selective hydrogenation using synthesized nanocatalysts are presented in Table 2.

Table 2. Testing of the catalysts in DHL hydrogenation

Catalyst	Pd loading, % (wt.)	TOF, mol DHL/ (mol Pd·s)	Selectivity (conversion), %
PS-b-P4VP-Pd	0.036	18.5	99 (100)
PS-b-P4VP-PdAu		36.9	99 (100)
PS-b-P4VP-PdZn		34.4	98 (100)
PS-b-P4VP-PdPt		49.2	98 (100)
PS-b-P4VP-Pd/Al_2O_3		34.0	98 (100)
PS-b-P4VP-PdAu/Al_2O_3		14.8	98 (100)
PS-b-P4VP-PdZn/Al_2O_3		52.2	99 (100)
PS-b-P4VP-PdPt/Al_2O_3		16.4	97 (100)
PEO-b-P2VP-Pd	0.060	9.6	98 (100)
PEO-b-P2VP-Pd/Al_2O_3		7.9	96 (100)
Pd-CS	0.370	4.0	98 (100)
Pd-PSC-1	0.230	4.9	95 (100)
Pd-PSC-2	0.300	4.0	94 (98)
Pd-PSC-3	0.300	4.4	94 (99)
Pd-PSC-4	0.250	2.9	95 (98)
Pd-PSC-5	0.220	4.9	94 (100)
Pd-PDADMAC	0.580	4.5	98 (98)
HPS-Pd	0.050	1.7	96 (100)
HPS-Pd/Zn		2.0	99 (100)

During the investigation of PS-b-P4VP colloids it was revealed that for Pd-Au colloids only one kind of active centers existed, while for Pd, Pd-Pt, and Pd-Zn colloids, there are at least two types of active centers. It was assumed that bimetallic NPs have different structure: Pd-Au – core-shell and Pd-Pt – cluster in cluster. In the case of Pd-Zn colloids there were both Pd atoms and Zn ions on the catalytic surface (according to the data of FTIRS of CO adsorption and XPS analyses) [5]. As it can be seen from Table 2 the TOFs of bimetallic colloids are higher than for monometallic one, which can be explained by modifying influence of Au, Pt and Zn caused by the ligand and ensemble effects. For Pd-Au catalyst the higher TOF is due to the defects on the particle surface generated by formation of core-shell structure and by the fact that all Pd atoms are on the surface and available for the substrate. Besides, the supported PS-b-P4VP-Pd/Al_2O_3 has almost twice the TOF compared to the unsupported one. It accounts for fact that in the case of heterogeneous catalyst the micellar aggregates are likely distributed on the support surface, and the accessibility of catalytic sites increases [30].

It is also noticeable that P4VP micelle cores can not only control the NPs size and size distribution but also provide a modification of the NPs surface due to electron donation to Pd from pyridine units, resulting in decreased strength of LN adsorption. This modification is rather permanent, thus high stability and selectivity is considered to be the important advantage of polymer-stabilized NPs [5].

In case of CS-containing PE nanocatalysts the use of "layer-by-layer" preparation method was found to provide the stronger attaching of CS due to the existence of negatively charged PSS on alumina surface [7]. Monolayered deposition was found to provide rather weak sorption of CS, which resulted in the washing-off of the layers during the reaction, and thus to the loss of the catalytic activity. The optimal amounts of PSS and CS providing the most uniform ultra thin layer formation as well as higher stability of Pd NPs were determined. Though the activity and selectivity of the catalysts of PSC series is similar, but they catalytic behavior during the repeated use is quite different. It was revealed that Pd-PSC-3 with equal content of both polycation CS and polyanion PSS has the best stability: activity remains almost the same while the selectivity even increases up to 97% [7].

For HPS-based catalysts it was found that the decrease of the electron density favors the double bonds hydrogenation, but in the case of the triple bonds the use of the catalysts with the higher surface electron density is preferable. Zn is known to be a donor related to Pd, so it is able to increase the electron density at the surface palladium atoms. So the modifier (Zn) introduction into the HPS catalyst was revealed to lead to the higher selectivity (Table 2) although the activity remained almost the same.

3.2 Direct Oxidation of Monosaccharides

The use of a selective catalyst for direct oxidation of D-glucose allowed us to maintain or even increase the productions (see Table 3) as well as to improve the quality of the end-products.

Table 3. Testing of the catalysts in D-glucose oxidation

Catalyst	Active metal loading, % (wt.)	TOF, mol S/ (mol Me · s) × 10^3	Selectivity*, %
PEO-b-P2VP-Pt-1	Pt-1.5	0.5	98
PEO-b-P2VP-Pt-1/Al_2O_3	Pt-1.5	1.0	99
PEO-b-P2VP-Pt-2	Pt-3.0	1.5	99
PEO-b-P2VP-Pt-2/Al_2O_3	Pt-3.0	1.5	99
PS-b-P4VP-Pt-1	Pt-1.5	0.3	99
PS-b-P4VP-Pt-1/Al_2O_3	Pt-1.5	1.0	99
PS-b-P4VP-Pt-2	Pt-3.0	0.8	97
PS-b-P4VP-Pt-2/Al_2O_3	Pt-3.0	0.5	98
HPS-Pd-1	Pd-1.0	0.7	99
HPS-Pd-2	Pd-3.0	1.6	99
HPS-Pd-3	Pd-5.0	3.3	99
HPS-Pt-1	Pt-1.0	1.0	99
HPS-Pt-2	Pt-3.0	2.8	99
HPS-Pt-3	Pt-5.0	5.0	98
HPS-Ru-1	Ru-0.5	3.0	98
HPS-Ru-2	Ru-1.0	8.0	99
HPS-Ru-3	Ru-3.0	7.0	95
HPS-Pd/Pt-1	Pd-0.5	0.3	98
HPS-Pd/Pt-2	Pd-1.0	1.8	97
HPS-Pd/Pt-3	Pd-2.0	2.1	98

*Selectivity of D-glucose oxidation is measured at 95% conversion

It is important to mention that for all the catalysts on the base of HPS metal NPs have mixed valence structure: for Pd – Pd(0) and Pd(II); for Pt – Pt(0),

Pt(II), and Pt(IV); and for Ru – Ru (0), Ru (IV) as anhydrous RuO_2 and $RuO_2 \cdot nH_2O$ and ruthenate ions $[RuO_x(OH)_y]^{z-}$, which allowed us assuming the mechanism similar to oxidation-reduction mechanism of Mars-van Krevelen, when lattice oxygen is responsible for catalytic activity and selectivity [34].

3.3 Phenol CWAO

Comparison of catalytic activity

Ru catalysts prepared by impregnation of different types of activated carbons exhibited enhanced activity in the CWAO of organic substances and especially in the phenol CWAO [3, 15]. This motivated us to compare catalytic properties of Ru-containing catalysts based on HPS and those based on activated carbon. The highest turnover frequency (TOF) of the phenol conversion was found for HPS-Ru(2.8%) and Ru/ACC(Fluka)-5% (was purchased from Fluka) while the other catalysts showed lower values (Table 4). Moreover, the lower the metal loading, the lower the TOF and conversion. Considering that the RuO_2 NP size is nearly the same in all the samples, the better catalytic performance of HPS-Ru(2.8%) can be ascribed to the larger amount of NPs, therefore, to the larger amount of catalytic sites.

The TOF values and the removal degrees for the Ru-containing HPS are higher than those for the Ru-containing catalyst based on zirconium oxide and similar to those for Ru-containing catalysts based on carbon supports [3, 15]. However, the Pt based HPS catalysts described in our preceding papers [6, 24, 28] exhibited lower activity (TOF $1.6 \div 7.3 \times 10^{-3}$ s^{-1}) compare to the HPS-Ru samples described here. The comparatively high activity of Ru-containing HPS catalysts can be associated with small RuO_2 NP size and high porosity of the parent HPS.

Table 4. The catalytic data for HPS based catalysts

Catalyst	TOF mol/(mol (Ru) s)*	Conversion %
Ru/ACC(Fluka)-5%	6.1×10^{-2}	95
HPS-Ru(2.8%)	6.2×10^{-2}	97
HPS-Ru(0.9%)	4.8×10^{-2}	89.0
HPS-Ru(0.5%)	3.2×10^{-2}	65.9

* $TOF = \frac{C(Phen) * \alpha}{C(Ru) * t * 100}$, where α is the conversion rate, %, and *t* is the time, hours.

Effect of phenol concentration

The influence of the phenol concentration on oxidation process was examined by varying the initial phenol concentration (C_o) from 0.05 mol(Phenol)/L to 0.42 mol(Phenol)/L. The kinetic curves of phenol conversion for Ru/ACC(Fluka)-5%, HPS-Ru(2.8%), and HPS-Ru(0.9%) are presented in Fig 6. It can be seen that increasing the phenol concentration results in increasing the phenol conversion rate for all tested catalysts.

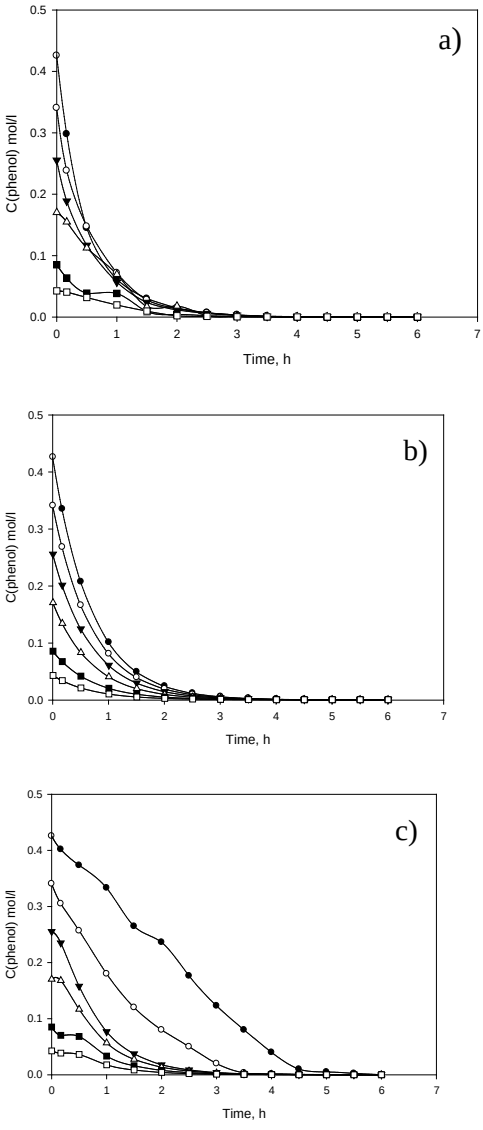

Fig. 6. The dependences of phenol concentration on time for different phenol initial concentrations for a) Ru/ACC(Fluka)-5%, b)Ru/HPS-2.8% c) Ru/HPS-0.9% (reaction conditions: P_{O2} 4.5 MPa; W_s 600 rpm, W_{O2} 10 mL/s)

Effect of the reaction temperature

The temperature is a key factor in the CWAO process because increasing the reaction temperature results in increasing the phenol conversion. To evaluate the influence of the temperature on the catalytic activity, the oxidation process was carried out in the temperature range 50-95 °C. As is shown in Fig 7, the higher temperature results in the higher TOF values.

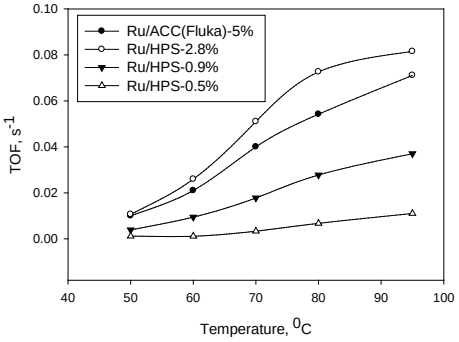

Fig. 7 Dependence of TOF of the CWAO process on temperature (reaction conditions: P_{O2} 4.5 MPa; W_s 600 rpm, W_{O2} 10 mL/s)

Effect of pH

To evaluate the dependence of phenol oxidation process on pH, the experiments were carried out in buffer solutions. Fig. 8 shows the effect of pH on the TOF and COD removal of phenol oxidation. Increasing the pH of the reaction solutions results in increasing the TOF while COD removal diminishes due to formation of intermediates and stabilization of acetic acid. The main intermediates that were detected at high pH values were maleic, succinic, fumaric, acrylic and pyruvic acids in the form of the corresponding salts.

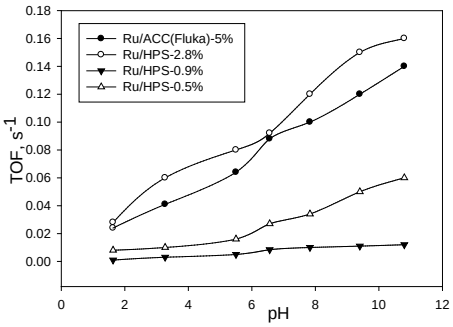

Fig. 8 The dependence of TOF on pH (reaction conditions P_{O2} 4.5 MPa; W_s 600 rpm, W_{O2} 10 mL/s)

At low pH values these intermediates are rapidly transform to acetic acid. Formation of large amounts of different acids results in active metal leaching and the decrease of the reaction rate, therefore rapid oxidation of the organic acids formed is the key factor for the enhanced catalyst stability in the CWAO processes.

Physicochemical characterization

TEM images of HPS-Ru(2.8%), HPS-Ru(0.9%), HPS-Ru(0.5%) and histograms of their particle size distributions are presented on Fig 9. For HPS-Ru(2.8%), the TEM image shows the existence of small nanoparticles with diameters in the range 0.5-2.5 nm with (a mean diameter of 1.4 nm). When the Ru content drops to 0.9 (for HPS-Ru(0.9%)), the mean NP diameter slightly decreases to 1.2 nm. A further decrease of the Ru content (HPS-Ru(0.5%)) does not influence the NP size. Thus, the NP diameter is nearly independent of the Ru loading revealing that the HPS nanopores restrict growth of the RuO_2 nanoparticles [35].

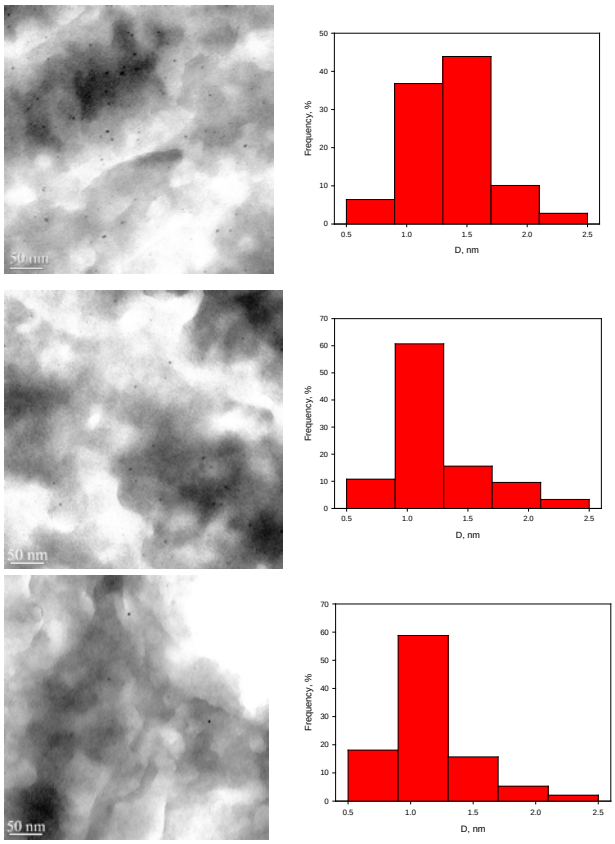

Fig . 9. TEM images and histograms of particle size distributions for a) Ru/HPS-2.8%, b) Ru/HPS-0.9%, and c) Ru/HPS-0.5%

X-ray photoelectron spectroscopy

The XPS data of the HPS-Ru(2.8%) and HPS-Ru(0.9%) samples are presented in Table 5. Because of the low Ru content in the HPS-Ru(0.5%) sample, the XPS data were not taken. Deconvolution of the X-ray photoelectron spectra reveals two different species with different binding energies, one of which at 463.3-462.9 eV can be ascribed to Ru(IV) in RuO_2 while the second one at 465.5-464.7 eV can be assigned to hydratated ruthenium oxide Ru(IV)×nH_2O. According to deconvolution of the XPS data provided in Table 5, after phenol oxidation the Ru $3p_{3/2}$ binding energies remain nearly unchanged, indicating catalyst structure stability.

Table 5 The biding energies of the Ru species in the catalysts studied

Catalyst	Ru $3p_{3/2}$, E_b, eV ± 0.1 eV		
	Ru(IV)	Ru(IV)·nH_2O	Ru(IV)/(Ru(IV)·nH_2O)
HPS-Ru(2.8%)	463.3	465.5	0.96
HPS-Ru(2.8%) OX*	462.9	464.7	1.2
HPS-Ru(0.9%)	462.9	464.7	0.99
HPS-Ru(0.9%) - OX*	462.9	464.7	0.99

*reaction conditions: reaction temperature 95^0C, oxygen flow rate 10 mL/min, oxygen pressure 4.5 MPa, phenol initial concentration 0.09 mol/L, catalysts loading 0.0016 mol(Ru)/L.

The ratio of Ru(IV) to (Ru(IV)×nH_2O) for HPS-Ru(2.8%) before oxidation is 0.96 while after the CWAO process the amount of Ru(IV) species increase by 24% and the ratio becomes 1.2. The ratio of Ru(IV) to (Ru(IV) ×nH_2O) for HPS-Ru(0.9%) remains unchanged (0.99) even after the CWAO process.

4 Conclusions

Investigated methods for nanocatalysts synthesis allowed developing highly active, selective (selectivity reached up to 99% at 100% conversion) and stable catalytic systems for oxidation and hydrogenation reactions. In polymeric systems, nanostructures were found to play the role of nanoreactors for the growing NPs. The possibility of the interaction of the catalytic active phase with solvent, support, modifier and substrate was revealed. For all investigated catalysts the interaction of active component with the solvent, support, modifier and substrate was found to take place. The diameter of NPs was determined by TEM, XRD and AFM to be equal to 2–3 nm.

We developed a series of catalysts based on HPS and RuO_2 nanoparticles. The formation of NPs is effectively restricted by the HPS nanopores. According to XPS, they contain two kinds of species: Ru(IV) and Ru(IV)×nH_2O and both species are stable during phenol oxidation. At the low active metal loading, practically no metal leaching was observed, while at the higher Ru content the metal leaching was minor. The catalytic activity and selectivity of the catalysts synthesized have been examined under a wide variety of reaction conditions. The most active catalyst was found to be HPS-Ru(2.8%). Compared to the commercial catalyst, Ru/ACC(Fluka)-5%, HPS-Ru(2.8%) allows similar activity and selectivity but at the lower Ru content, thus leading to significant savings of a noble metal.

Acknowledgements:

The authors thank Dr. L. M. Bronstein and her colleagues (Department of Chemistry, Indiana University, USA) for their help in carrying out TEM. Financial support for this investigation was provided by the Ministry of Education and Science of the Russian Federation and the Russian Foundation for Basic Research.

References:

[1] A. Wieckowski , E. R. Savinova , C. G. Vayenas, *Catalysis and Electrocatalysis at Nanoparticle Surfaces* , Marcel Dekker , New York , 2003 , pp. 970 .

[2] G. Schmid , *Nanoparticles: From Theory to Application* , Wiley - VCH , Weinheim , 2004 , pp. 434 .

[3] G. A. Somorjai , A. M. Contreras , M. Montano , R. M. Rioux. Clusters, Surfaces, and Catalysis. *Proc. Nat. Acad. Sci. USA* .Vol 103 , 2006, pp 10577-10583.

[4] D. Astruc, F. Lu, J.R. Aranzaes, Nanoparticles as Recyclable Catalysts: The Frontier between Homogeneous and Heterogeneous Catalysis, *Angewandte Chemie International Edition*, Vol 44, No 48, 2005, pp 7852-7872.

[5] L. Bronstein, D. Chernyshov, I. Volkov, M. Ezernitskaya, P. Valetsky, V. Matveeva, E. Sulman, Structure and Properties of Bimetallic Colloids

Formed in Polystyrene-block-Poly-4-vinylpyridine Micelles: Catalytic Behavior in Selective Hydrogenation of dehydrolinalool, *Journal of Catalysis*, Vol 196, No 2, 2000, pp 302-314.

[6] N.V. Semagina, A.V. Bykov, E.M. Sulman, V.G. Matveeva, S.N. Sidorov, L.V. Dubrovina, P.M. Valetsky, O.I. Kiselyova, A.R. Khokhlov, B. Stein, L.M. Bronstein, Selective Dehydrolinalool Hydrogenation with Poly(ethylene oxide)-*block*-Poly-2-vinylpyridine Micelles Filled with Pd Nanoparticles, *Journal of Molecular Catalysis A: Chemical*, Vol 208, No 1-2 , 2004, pp 273–284.

[7] I.B. Tsvetkova, L.M. Bronstein, S.N. Sidorov, O.L. Lependina, M.G. Sulman, P.M. Valetsky, B. Stein, L.Zh. Nikoshvili, V.G. Matveeva, A.I. Sidorov, B.B. Tikhonov, G.N. Demidenko, L. Kiwi-Minsker, E.M. Sulman. Structure and behavior of nanoparticulate catalysts based on ultrathin chitosan layers, *Journal of Molecular Catalysis A: Chemical*, Vol 276, No 1-2, 2007, pp 116–129.

[8] L.M. Bronstein, V.G. Matveeva, E.M. Sulman, Nanoparticulate Catalysts Based on Nanostructured Polymers, *Nanoparticles and Catalysis* (Ed.: Astruć, D). – Wiley-VCH GmbH & Co. KGaA, Weinheim, 2007, pp 93-127.

[9] Mahdi Shahmiri, Nor Azowa Ibrahim, Norhazlin Zainuddin, Nilofar Asim, B. Bakhtyar, A. Zaharim, K.Sopian. Effect of pH on the Synthesis of CuO Nanosheets by Quick Precipitation Method. *WSEAS TRANSACTIONS on ENVIRONMENT and DEVELOPMENT*, Vol 6, No 2, 2013, pp 243-252.

[10] L. Oliviero, J. Barbier Jr, D. Duprez, H. Wahyu, J.W. Ponton, I.S. Metcalfe and D. Mantzavinos, Wet air oxidation of aqueous solutions of maleic acid over Ru/CeO2 catalysts, *Applied Catalysis B: Environmental*, Vol 35, 2001, pp 1-12.

[11] E. Castillejos-Lopez, A. Maroto-Valiente, D.M. Nevskaia, V. Munoz, I. Rodriguez-Ramos and A. Guerrero-Ruiz, Methane combustion over supported palladium catalysts: I. Reactivity and active phase. *Catalysis Today*, Vol 143, No 3-4, 2009, pp 355-363.

[12] M. Besson, J.-C. Beziat, B. Blanc, S. Durecu, P. Gallezot, Treatment of aqueous solutions of organic pollutants by heterogeneous catalytic wet air oxidation (CWAO), Studies in Surface Science and Catalysis, Vol 130, 2000, pp 1553-1558.

[13] H. Delmas, C. Creanga, C. Julcour-Lebigue and A.M. Wilhelm, A sequential oxidative process for water treatment— Adsorption and batch CWAO regeneration of activated carbon, *Chemical Engineering Journal*, Vol 152, No 1, 2009, pp 189-194.

[14] O.Qteishat, S. Myszograj, M. Suchowska-Kisielewicz. Changes of wastewater characteristic during transport in sewers. *WSEAS TRANSACTIONS on ENVIRONMENT and DEVELOPMENT*, Vol 7, No 11, 2011, pp349-358.

[15] F. Arena, C. Italiano and L. Spadaro, Efficiency and reactivity pattern of ceria-based noble metal and transition metal-oxide catalysts in the wet air oxidation of phenol, *Applied Catalysis B: Environmental*, Vol 115-116, 2012, pp 336-345.

[16] J. Gaálová, K. Jirátová, J. Klempa, O. Šolcová, I. Maupin, J. Mijoin, P. Magnoux, J. Barbier, Jr. Zeolite and Mixed Oxide Catalysts for VOCs Oxidation. *WSEAS TRANSACTIONS on ENVIRONMENT and DEVELOPMENT*, Vol 10, 2014, pp 135-144.

[17] M. Martin-Hernandez, J. Carrera, M.E. Suarez-Ojeda, M. Besson and C. Descorme, Catalytic wet air oxidation of a high strength p-nitrophenol wastewater over Ru and Pt catalysts: Influence of the reaction conditions on biodegradability enhancement, *Applied Catalysis B: Environmental*, Vol 123-124, 2012, pp 141-150.

[18] I. Quesada-Penate, C. Julcour-Lebigue, U.J. Jauregui-Haza, A.M. Wilhelm and H. Delmas, *Journal of Hazardous Materials*, Vol 221-222, 2012, pp 131-138.

[19] A. Vallet, M. Besson, G. Ovejero and J. Garcia, Treatment of a non-azo dye aqueous solution by CWAO in continuous reactor using a Ni catalyst derived from hydrotalcite-like precursor, *Journal of Hazardous Materials*, Vol 227-228, 2012, pp 410-417.

[20] S. Yang, X. Wang, H. Yang, Y. Sun and Y. Liu, Influence of the different oxidation treatment on the performance of multi-walled carbon nanotubes in the catalytic wet air oxidation of phenol, *Journal of Hazardous Materials*, Vol 233-234, 2012, pp 18-24.

[21] C.D. Taboada, J. Batista, A. Pintar, J. Levec, Preparation, characterization and catalytic properties of carbon nanofiber-supported Pt, Pd, Ru monometallic particles in aqueous-phase reactions, *Applied Catalysis B*, Vol 89, No 3-4, 2009, 375-382.

[22]. M. Triki, Z. Ksibi, A. Ghorbel, F. Medina, Preparation and characterization of CeO_2–TiO_2 support for Ru catalysts: Application in CWAO of *p*-hydroxybenzoic acid, *Microporous and Mesoporous Materials*, Vol 117, No 1-2, 2009, pp 431-435.

[23] L. Oliviero, J.Ir. Barbier, D. Duprez, A. Guerrero-Ruiz, B. Bachiller-Baeza, I. Rodriguez-Ramos, Catalytic wet air oxidation of phenol and acrylic acid over Ru/C and Ru-CeO2/C catalysts, *Applied Catalysis B*, Vol 25, 2000, pp 267-275.

[24] N. Li, C. Descorme, M. Besson, Catalytic wet air oxidation of chlorophenols over supported ruthenium catalysts *Journal of Hazardous Materials*, Vol 146, 2007, pp 602-609.
[25] Arena F, Italiano C, Raneri A, Saja C Mechanistic and kinetic insights into the wet air oxidation of phenol with oxygen (CWAO) by homogeneous and heterogeneous transition-metal catalysts, *Applied Catalysis B*, Vol 99, No 1-2, 2010, pp 321-328.
[26] J.Y. Park, Y. Zhang, S.H. Joo, Y. Jung, G.A. Somorjai, Size effect of RhPt bimetallic nanoparticles in catalytic activity of CO oxidation: Role of surface segregation, *Catalysis Today*, Vol 181, pp 133-137.
[27] B.P. Vinayan, R.I. Jafri, R. Nagar, N. Rajalakshmi, K. Sethupathi, S. Ramaprabhu Catalytic activity of platinum–cobalt alloy nanoparticles decorated functionalized multiwalled carbon nanotubes for oxygen reduction reaction in PEMFC, *International Journal of Hydrogen Energy*,Vol 37, No 1, pp 412-421.
[28] H. Zhang, N. Toshima, Preparation of novel Au/Pt/Ag trimetallic nanoparticles and their high catalytic activity for aerobic glucose oxidation, *Applied Catalysis A*, Vol 400, No 1-2, 2011, pp 9-13.
[29] W-M. Liu, Y-Q. Hu, S-T. Tu Active carbon–ceramic sphere as support of ruthenium catalysts for catalytic wet air oxidation (CWAO) of resin effluent, *Journal of Hazardous Materials*, Vol 179, No 1-3, 2010, pp 545-551.
[30] E.M. Sulman, V.G. Matveeva, M.G. Sulman, G.N. Demidenko, P.M. Valetsky, B. Stein, T. Mates, L.M. Bronstein, Influence of Heterogenization on Catalytic Behavior of Mono- and Bimetallic Nanoparticles Formed in Poly(styrene)-*block*-Poly(4-vinylpyridine) Micelles, *Journal of Catalysis*, Vol 262, No 1, 2009, pp 150–158.
[31] E. Guibal, Heterogeneous Catalysis on Chitosan-Based Materials: a Review, *Progress in Polymer Science*, Vol 30, No 1, 2005, pp 71-109.
[32] S. Kidambi, M.L. Bruening, Multilayered Polyelectrolyte Films Containing Palladium Nanoparticles: Synthesis, Characterization, and Application in Selective Hydrogenation, *Chemistry of Materials*, Vol 17, No 2, 2005, pp 301-307.
[33] S.N. Sidorov, L.M. Bronstein, V.A. Danakov, M.P. Tsyurupa, S.P. Solodovnikov, P.M. Valetsky, E.A. Wilder, R.J. Spontak, Cobalt Nanoparticle Formation in the Pores of Hypercrosslinked Polystyrene: Control of Nanoparticle Growth and Morphology, *Chemistry of Materials*, Vol 11, No 11 , 1999, pp 3210-3215.
[34] E. Sulman, V. Doluda, S. Dzwigaj, E. Marceau, L. Kustov, O. Tkachenko, A. Bykov, V. Matveeva, M. Sulman, N. Lakina, Catalytic Properties of Ru Nanoparticles Introduced in a Matrix of Hypercrosslinked Polystyrene toward the Low Temperature Oxidation of D-Glucose, *Journal of Molecular Catalysis A: Chemical*, Vol 278, No 1-2, 2007, pp 112–119.
[35] V. Yu. Doluda , E. M. Sulman, V. G. Matveeva, M. G. Sulman, A. V. Bykov, N. V. Lakina, A. I. Sidorov, P. M. Valetsky • L. M. Bronstein, Phenol catalytic wet air oxidation over Ru nanoparticles formed in hypercrosslinked polystyrene, *Topics in Catalysis*, Vol 56, No 9-10, 2013, pp. 688-695.